Rapid Communications

van der Waals screening by graphenelike monolayers

Xiaofei Liu,* Zhuhua Zhang, and Wanlin Guo†

Key Laboratory for Intelligent Nano Materials and Devices of Ministry of Education, State Key Laboratory of Mechanics and Controlof Mechanical Structures, Nanjing University of Aeronautics and Astronautics, Nanjing 210016, China

(Received 28 February 2018; revised manuscript received 17 May 2018; published 28 June 2018)

The ubiquitous van der Waals (vdW) interaction determines the fundamental properties of material surfaces. Here, we show that graphene can partly screen the vdW energy by up to 53%, as tested in a graphene trilayer and a sandwiched BN/graphene/BN multilayer using the random phase approximation and density functional theory based many-body-dispersion method. The vdW screening turns weaker in semiconducting and insulating graphenelike monoatomic layers, displaying a strong correlation with the band gap and the dielectric constant of materials, but depends less on the screened materials. The revealed relationship between the vdW screening and the fundamental electronic structure of the graphenelike material will be instrumental in the rational control of surface interactions.

DOI: 10.1103/PhysRevB.97.241411

Planar graphenelike monoatomic layered crystals, with properties spanning from insulators, semiconductors, to semimetals, are the thinnest group of crystalline materials in nature [1–6]. Their atomic thickness, along with novel physical properties, make these monolayers promising for applications in nanoscale electronic devices. For instance, graphene has been used in high cutoff frequency transistors due to its massless Dirac fermion, while monolayer hexagonal boron nitride (BN) could serve as an ideal atomically flat substrate for high-performance graphene devices [7,8]. In addition, planar graphenelike monolayers provide natural, ultrathin, and flat membranes that are suited for many applications. Successful examples include electricity generation in graphene by interactions with rain droplets, the anticorrosion coatings of metal surfaces, gas filters with perforated graphene, and ultrathin mechanical oscillators [9–12]. In all those applications, the planar monolayers have to make contact with substrates, electrodes, and other species, dominantly through a van der Waals (vdW) interaction or a so-called dispersion interaction.

Any adsorbate or material on graphenelike monolayers is subjected to the vdW interaction, which dominates many fundamental phenomena, such as gas absorption, wetting, and the assembly of vdW crystals [13–18]. Meanwhile, the unavoidable substrate underneath the monolayer poses an additional vdW interaction to the adsorbent or material. The substrate and monolayer together make the vdW interaction quite complicated in those systems. Existing theoretical studies often simplify the substrate as a slab made of a few atomic layers or even directly neglect the interaction between the substrate and adsorbate, as the vdW interaction between the top monolayer and adsorbate is thought to be dominant when they are closely contacted. However, the effect of the substrate is indispensable in longer ranges, since the vdW energy versus distance L scales as L^{-4} in monolayer-related systems, instead of L^{-2} in bulk-related systems [19]. Molecular dynamics simulations have been employed to investigate the effect of a substrate on the wetting behaviors of the monolayers, yet yielding controversial results on whether the substrate can influence the wetting performance [20–23]. A possible issue lies in that those studies fully account the vdW energy between the substrate and object on the monolayer into the total energy, but neglect a possibility of vdW screening by the intermediate monolayer, in a manner similar to the Coulomb screening [24–27]. Given the ubiquity of the vdW interaction between low-dimensional structures and that the widely studied graphenelike monolayers have to be bolstered by substrates, it is urgent to fully understand the possible vdW screening. Several fundamental questions naturally arise: Could the vdW energy be effectively screened by graphenelike monolayers? If so, to what extent could the vdW energy be screened? What determines the extent?

In this Rapid Communication, we address above questions via applying the state-of-art random phase approximation in prototype models of homogeneous and heterogeneous trilayers. In agreement with a recent experimental observation in a tip/graphene/substrate system [28], the graphene monolayer can indeed screen the vdW interaction, but the screening is limited to a ratio of 53%. Through analyzing the screening capabilities of nine semiconducting or insulating planar graphenelike monolayers, we show a correlation of the vdW screening capability with the direct band gap and dielectric constant of the monolayer, as well as secondary effects from the screened materials. Consistent with its semimetallic nature, graphene is found to be superior to other semiconducting or insulating atomistic monolayers in giving a large ratio of vdW screening. In addition, we demonstrate the importance of vdW screening by graphene in realistic systems, the graphene/graphene/silicon (Gr/Gr/silicon) and benzene/graphene/graphene (benzene/Gr/Gr) heterostructures.

The vdW interaction originating from quantum mechanical fluctuations of electromagnetic fields is a many-body collective effect. Practices teach that when the interval between two

*liuxiaofei@nuaa.edu.cn
†wlguo@nuaa.edu.cn

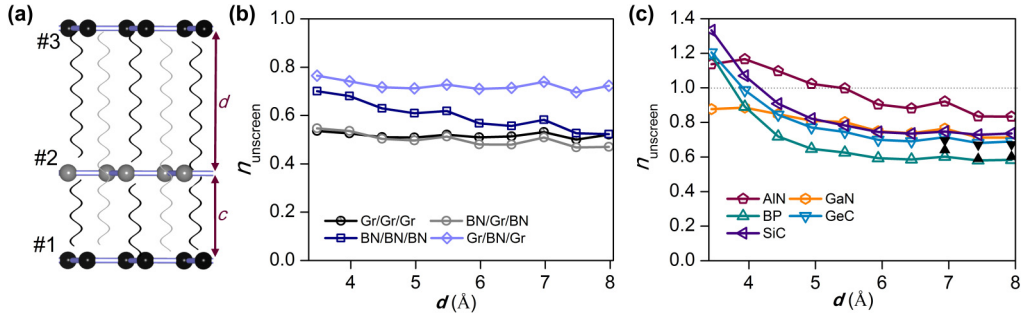

FIG. 1. vdW energy screening in the AB/CA/AB stacked homogeneous/heterogeneous graphenelike trilayers of an asymmetric configurations. (a) Illustration of the asymmetric configuration of the trilayer. The interlayer distance c is fixed to 3.4 Å, whereas d varies in the range from 3.4 to 7.9 Å. The black and gray wavy lines denote the vdW interactions without and with screening, respectively. (b) The ratio of unscreened vdW energy n_{unscreen} as a function of d, calculated by the ACFDT-RPA. (c) n_{unscreen} as a function of d in the AlN, GaN, BP, GeC, and SiC homogeneous trilayers. n_{unscreen} in the heterogeneous AlN/BP/AlN and BP/GeC/BP is labeled by the black up and down triangles, respectively.

objects is filled with a dielectric medium instead of the vacuum, the vdW energy would be significantly reduced, suggesting an effect of vdW screening [19,29]. It is not appropriate to describe the vdW screening due to an atomic monolayer by a single constant, as the many-body effect depends on detailed environments. However, using effective Hamaker constants due to screening as in a recent experiment [28] benefits straightforward experimental explanations and understandings. To calculate the capability of vdW screening of graphenelike monolayers, we employ the adiabatic-connection fluctuation-dissipation theorem with the random phase approximation (ACFDT-RPA), which is reliable among the computationally feasible theories for correlation energy calculations in molecular crystals, vdW crystals, and solids [30–33]. Since it is extremely expensive to simulate the tip/graphene/substrate system by the ACFDT-RPA, prototype models of homogeneous and heterogeneous trilayers are adopted, as illustrated in Figs. 1(a) and 2(a). First, the RPA correlation energies of the trilayers, bilayers, and monolayers are calculated. The vdW energy between layer No. 3 and bilayers No. 2 and No. 1, E_{tri}, is defined as the correlation energy difference between the trilayer and the isolated layer No. 3 and bilayers No. 2 and No. 1. Likewise, the vdW energy between any two layers is defined as the correlation energy difference between the bilayer and corresponding isolated layers. Then, the ratio of unscreened vdW energy between layers No. 1 and No. 3 is written as $n_{\text{unscreen}} = \frac{E_{\text{tri}} - E_{\text{bi}}}{E_{\text{bi}'}}$, where E_{bi} ($E_{\text{bi}'}$) denotes the vdW energy between layers No. 3 and No. 2 (layers No. 3 and No. 1) in the corresponding bilayer without the third layer. In this definition, it is assumed that the vdW energy between layers No. 3 and No. 2 is not influenced by layer No. 1 underneath, while the many-body nature of the vdW interaction is fully captured by the screening effect due to the middle layer.

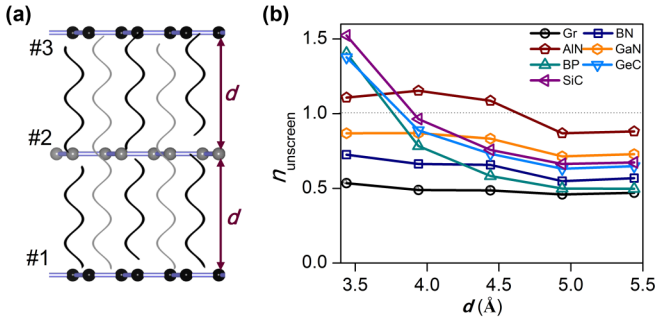

FIG. 2. vdW energy screening in the AB/CA/AB stacked homogeneous planar graphenelike trilayers of a symmetric configuration. (a) The symmetric simulation configuration of the trilayer. (b) The ratio of unscreened vdW energy as a function of interlayer distance d, calculated by the ACFDT-RPA.

The ACFDT-RPA calculations were performed with the projector augmented-wave method using the VASP code [34]. The orbitals of Kohn-Sham formulism were calculated with the Perdew-Burke-Ernzernhof (PBE) functional [35], using k-point meshes of $11\times11\times1$ for graphene and BN, and $10\times10\times1$ for all other monoatomic layers. A kinetic energy cutoff of 400 eV was adopted for the plane-wave expansion and the primitive cells with a perpendicular dimension of 30 Å were used to avoid any spurious interaction between period images. The density functional theory (DFT) calculations with the many-body-dispersion correction (PBE+MBD) were performed with a k-point mesh of $19\times19\times1$. In all calculations, the homogeneous or heterogeneous trilayers were AB/CA/AB stacked. The lattice constants of graphene and BN were set to be 2.46 Å, whereas those of AlN, BP, SiC, GaN, and GeC were set to be 3.15 Å with negligible misfit strains, for the convenience of building heterostructures. The lattice constants of SnC, BAs, and InN were fully relaxed using the PBE functional. To calculate the static dielectric constants, the random phase approximation was applied without a local field effect, with an effective thickness of 2 Å for all the monolayers.

We mainly investigate the vdW screening at short ranges due to the limitation of computational costs. For the asymmetric configuration shown in Fig. 1(a), the layer distance between the middle layer No. 2 and bottom layer No. 3 is fixed to 3.4 Å, with the interlayer distance d between the middle layer No. 2 and top layer No. 1 varying from 3.4 to 7.9 Å. For the symmetric configuration in Fig. 2(a), the interlayer distance d varies from 3.4 to 5.4 Å. The ratio of unscreened vdW energy between the top and bottom layers in the graphene, BN, and heterogeneous trilayers is illustrated in Fig. 1(b) as a function of distance. Generally, the ratio of unscreened vdW, n_{unscreen}, in the trilayers of graphene and BN is lower than 1, justifying that the graphenelike monolayers indeed screen vdW interactions.

In the homogeneous graphene trilayer, n_{unscreen} within the studied distances is in the narrow range from 0.50 to 0.54, indicating that the screening of vdW energy by graphene can be well described by a constant. In the heterogeneous trilayers, BN/Gr/BN [Fig. 1(b)], Gr/Gr/BN, and BN/Gr/Gr trilayers (Fig. S1 in the Supplemental Material [36]), n_{unscreen} is close to that in the homogeneous case regardless of the screened materials, which is a hint for the robust screening capability of graphene. The incomplete screening of vdW energy by graphene observed here is at odds with the report of complete screening in the experiment [28]. Theoretically, to completely screening vdW interactions, a medium with an infinitely large dielectric function is required to fully screen the Coulomb interaction. However, graphene has a finite dielectric function at small q vectors, and the real part of dielectric function in graphene significantly reduces with an increased magnitude of the q vector [37,38], further attenuating the screening effect. The inconsistency between the perfect screening reported by Tsoi *et al.* [28] and the incomplete screening here could stem from the effect of charge doping in the experiment, as previous theoretical works found that charge doping enhances the electron screening in graphene such as to reduce the binding energy of exciton [39,40].

The vdW screening capability of the BN monolayer exhibits a pronounced distance dependence. As d increases, n_{unscreen} in the homogeneous BN trilayer decreases from 0.70 to 0.53 and tends to converge at a sufficiently large distance. Although n_{unscreen} of BN at $d = 7.9$ Å (0.53) is close to that in the graphene trilayer, in the heterogeneous Gr/BN/Gr [Fig. 1(b)], Gr/BN/BN, and BN/BN/Gr trilayers (Fig. S1 [36]), the screening capability of BN is much weaker. When both layers No. 1 and No. 2 are graphene, n_{unscreen} of BN is 0.72, and when they are graphene and BN, respectively, n_{unscreen} of BN is in between those values. Thus, the screening capability of BN is stronger for the vdW interaction between BN layers than that between graphene layers. Though there are secondary effects from the screened materials, the middle layer dominates the screening, as the middle BN layer always exhibits a screening capability weaker than the middle graphene layer, regardless of the screened materials.

Figure 1(c) shows the ratio of unscreened vdW energy as a function of distance in the other five homogeneous trilayers, AlN, GaN, BP, GeC, and SiC. For GaN, n_{unscreen} is lower than 1 in the considered distances. Similar to the case of BN, n_{unscreen} in the GaN trilayer exhibits a distance dependence, decreasing from 0.88 at $d = 3.4$ Å to 0.71 at $d = 7.9$ Å. The other four monolayers exhibit abnormal screening behaviors at small distances. With d ranging from 3.4 to 3.9 Å in BP, GeC, and SiC, and from 3.4 to 4.9 Å in AlN, n_{unscreen} exceeds 1. This abnormal "negative screening" could stem from the larger atomic radii of Al, Ge, Si, P, and the ensuing slight charge redistributions at the interfaces (Fig. S2 [36]). Nevertheless, n_{unscreen} reduces to be lower than 1 as d increases and converges at $d = 7.9$ Å, complying with the definition of the screening ratio. In the heterogeneous Al/BP/Al and BP/Ge/BP trilayers, n_{unscreen} is close to that in the homogeneous BP and Ge trilayers, further verifying the dominant role of the middle layer.

To demonstrate the robustness of the screening capability of graphenelike monolayers, a symmetric configuration of the homogeneous trilayers is also simulated. As illustrated in Fig. 2, the main picture of the vdW screening is preserved upon the change of relative interlayer distances. In the graphene, BN, and GaN trilayers, n_{unscreen} is lower than 1 in the studied range of distances, whereas AlN, BP, GeC, and SiC still exhibit negative screening when the layers are too close to each other [Fig. 2(b)]. As expected, no essential deviation of n_{unscreen} at $d = 5.4$ Å in the symmetric configuration from the converged value in the asymmetric case is found. For instance, n_{unscreen} in the two cases of BN are 0.57 and 0.53, respectively. The only difference observed is the fast convergence of n_{unscreen} when both layers No. 3 and No. 1 depart from the middle layer.

TABLE I. The direct PBE band gap E_{dir}, static in-plane dielectric constant ε of the monolayer, and ratio of unscreened vdW energy of the asymmetric configuration n_{unscreen} at $d = 7.9$ Å and of the symmetric configuration $n_{\text{unscreen}'}$ at $d = 5.4$ Å. The dielectric constant is defined as $\varepsilon = 1 + \frac{L(\varepsilon_{\text{cal}}-1)}{T}$, where T is the effective thickness of monolayer, L is the thickness of vacuum slab, and ε_{cal} is the dielectric constant of the monolayer within the vacuum slab.

	Gr	BN	AlN	BP	SiC	GaN	GeC	SnC	BAs	InN
E_{dir} (eV)	0.00	4.90	3.54	0.85	2.39	2.73	2.29	1.70	0.72	0.78
ε	29.7	7.3	7.0	34.3	15.9	8.8	16.6	22.0	37.2	23.8
n_{unscreen}	0.52	0.53	0.83	0.58	0.74	0.71	0.69	0.66	0.56	0.53
$n_{\text{unscreen}'}$	0.47	0.57	0.88	0.50	0.67	0.73	0.65	0.57	0.44	0.67

The ratios of unscreened vdW energy at the largest considered distances in the asymmetric and symmetric configurations are listed in Table I, along with the PBE direct band gaps and static in-plane dielectric constants of the monolayers. All n_{unscreen} ($n_{\text{unscreen}'}$) are found to be lower than 1, implying the positive vdW screening by all these monolayers. Notably, graphene has the strongest screening capability in the asymmetric case, whereas the BAs monolayer stands out in the symmetric case. The AlN monolayer is a relatively poor vdW screening material, which screens 17% and 12% vdW energy in the asymmetric and symmetric cases, respectively.

To gain a deeper insight into the material dependence of vdW screening capability, the n_{unscreen}-band-gap relationship is depicted in Fig. 3(a). Interestingly, the monolayer with a smaller band gap tends to have a stronger vdW screening capability. For instance, graphene, BAs, and InN have a band gap of 0.00, 0.72, and 0.78 eV, relatively smaller compared to the others, which explains their small ratios of unscreened vdW energy (0.52, 0.56, and 0.53, respectively). In contrast, the poor vdW screening material AlN has a wide band gap of 3.54 eV. As illustrated in Fig. 3(b), the screening capability of the monolayer also correlates with the static in-plane dielectric constant. A high dielectric constant of a monolayer corresponds to a strong vdW screening capability, since this constant is often an indicator of the size of the band gap. Moreover, this trend informs a zero vdW screening for a material with a dielectric constant of vacuum. The observed correlation to the band gap and dielectric constant is in good accordance with the fact that insulators with large band gaps have weaker screening effects on Coulomb interactions. Considering the large band gap (4.90 eV) and small in-plane dielectric constant (7.3), the vdW screening capability of the BN monolayer is unexpectedly high in the BN trilayer. Nevertheless, when the screened material is graphene, BN leads to a much weaker screening, consistent

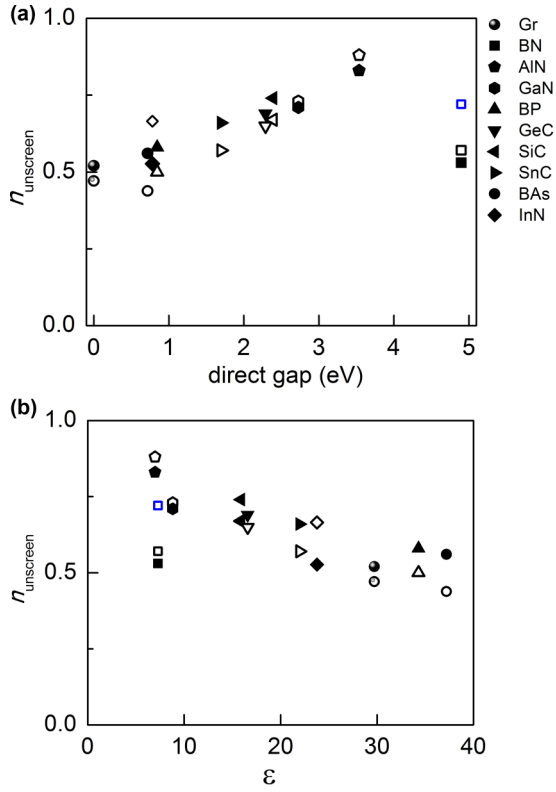

FIG. 3. The ratio of unscreened vdW energy as a function of (a) the direct PBE band gap and (b) static in-plane dielectric constant, for $d = 7.9$ Å in the asymmetric configuration (open scatters) and $d = 5.4$ Å in the symmetric configuration (solid scatters). n_{unscreen} in the Gr/BN/Gr is labeled by the blue square.

with its insulating nature. We note that the Lifshitz theory [24,29] using an effective dielectric environment between the top and bottom monolayers could help qualitatively understand the vdW screening in the trilayers.

The DFT-based MBD method that intimately links to the RPA theory includes the many-body effect of the vdW interaction in a computationally friendly manner [41–46]. Figure 4(a) illustrates n_{unscreen} in the homogeneous trilayers calculated by the PBE+MBD. In the graphene trilayer with an asymmetric configuration, the trend slightly deviates from that by the ACFDT-RPA, as n_{unscreen} first increases from 0.95 at $d = 3.4$ Å to 0.98 at $d = 4.0$ Å but decreases thereafter to

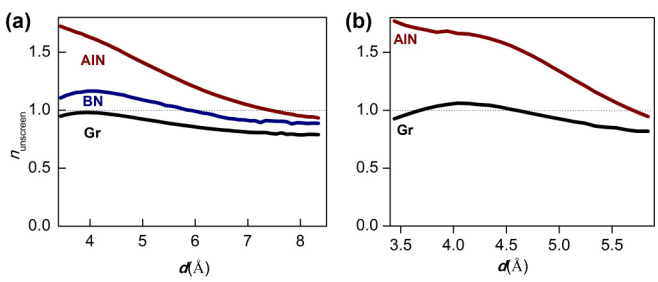

FIG. 4. The ratio of unscreened vdW energy in the AB/CA/AB stacked trilayers of the (a) asymmetric and (b) symmetric configurations, calculated by the PBE+MBD.

0.79 at $d = 8.4$ Å. In the symmetric case, a negative screening at $d \cong 4$ Å is predicted, which contradicts the ACFDT-RPA result. In the AlN trilayers, a negative screening is predicted in a wider range of d (from 3.4 to 7.4 Å in the asymmetric case), while n_{unscreen} at $d = 8.4$ Å is 0.93. Similar phenomena predicted in the other monolayers are presented in Fig. S4 [36]. In short, the PBE+MBD method qualitatively gives the tendency of vdW screening as a function of distance, but underestimates the screening capabilities of the monolayers. Another difficulty for the PBE+MBD method is to predict the relative screening capabilities of different materials, as it leads to a stronger vdW screening by GeC and SiC than by graphene in contrast to the trend revealed by the ACFDT-RPA. This issue arises because the MBD method approximates the vdW energy using coupled quantum harmonic oscillators instead of exact electronic structures. Nevertheless, the PBE+MBD method is suited for a qualitative estimation of the vdW screening in practical situations. As shown in Fig. S5(a) [36], in a Gr/Gr/silicon heterogeneous system, when the top graphene layer departs from the equilibrium position by 0–3 Å, the ratio of screened vdW energy between the top graphene layer and the bottom silicon substrate can be up to ∼20%, underscoring the importance of vdW screening by monolayer graphene in realistic systems. In a benzene/Gr/Gr system, the middle layer exhibits a negative screening at the shortest distances.

To conclude, first-principles calculations with the random phase approximation were used to reveal the incomplete vdW screening by planar graphenelike monolayers. In the homogeneous or heterogeneous planar graphenelike trilayers, the ratio of screened vdW energy shows a correlation with the band gap and dielectric constant of the middle screening layer, with secondary effects from the screened materials. Though no perfect vdW screening is allowed, graphene has the strongest vdW screening capability among the ten considered planar graphenelike crystals. This finding would be instrumental to the understanding of the substrate-dependent behaviors of planar graphenelike monolayers. For instance, the substrate underneath would neither be transparent nor deterministic to the wetting of water on the graphene monolayer. In the jump-to-contact-retract test by an atomic force microscope, the screening capabilities of the monolayers would be crucial for both the jump-to-contact force and detaching force of the tip, if the monolayer could not fully screen the vdW interaction between the tip and substrate. We call for experimentalists to confirm the revealed band-gap dependence of vdW screening by planar graphenelike monolayers.

This work is supported by National Natural Science Foundation of China (11702132, 51535005, 11772153, and 51472117). X.L. is thankful for support from China Postdoctoral Science Foundation (No. 2016M600408 and No. 2017T100362) and the Natural Science Foundation of Jiangsu Province (No. BK20170770). Z.Z. is grateful to the Research Fund of State Key Laboratory of Mechanics and Control of Mechanical Structures (MCMS-0416K01, MCSM-0416G01, MCSM-0417G01, MCSM-0417G02, MCSM-0417G03) and the Fundamental Research Funds for the Central Universities (NP2017101, NC2018001, NE2018002).

[1] A. K. Geim and K. S. Novoselov, Nat. Mater. **6**, 183 (2007).
[2] A. H. Castro Neto, A. F. Guinea, N. M. R. Peres, K. S. Novoselov, and A. K. Geim, Rev. Mod. Phys. **81**, 109 (2009).
[3] Z. Liu, L. Song, S. Zhao, J. Huang, L. Ma, J. Zhang, J. Lou, and P. M. Ajayan, Nano Lett. **11**, 2032 (2011).
[4] J. Yin, X. Liu, W. Lu, J. Li, Y. Cao, Y. Li, Y. Xu, X. Li, J. Zhou, C. Jin, and W. Guo, Small **11**, 5375 (2015).
[5] A. Fleurence, R. Friedlein, T. Ozaki, H. Kawai, Y. Wang, and Y. Yamada-Takamura, Phys. Rev. Lett. **108**, 245501 (2012).
[6] H. Şahin, S. Cahangirov, M. Topsakal, E. Bekaroglu, E. Akturk, R. T. Senger, and S. Ciraci, Phys. Rev. B **80**, 155453 (2009).
[7] Y. M. Lin, C. Dimitrakopoulos, K. A. Jenkins, D. B. Farmer, H.-Y. Chiu, A. Grill, and Ph. Avouris, Science **327**, 662 (2010).
[8] C. R. Dean, A. F. Young, I. Meric, C. Lee, L. Wang, S. Sorgenfrei, K. Watanabe, T. Taniguchi, P. Kim, K. L. Shepard, and J. Hone, Nat. Nanotechnol. **5**, 722 (2010).
[9] J. Yin, X. Li, J. Yu, Z. Zhang, J. Zhou, and W. Guo, Nat. Nanotechnol. **9**, 378 (2014).
[10] Z. Zhang, J. Yin, X. Liu, J. Li, J. Zhang, and W. Guo, J. Phys. Chem. Lett. **7**, 867 (2016).
[11] S. P. Koenig, L. Wang, J. Pellegrino, and J. S. Bunch, Nat. Nanotechnol. **7**, 728 (2012).
[12] M. Ganzhorn, S. Klyatskaya, M. Ruben, and W. Wernsdorfer, ACS Nano **7**, 6225 (2013).
[13] L. Zhao, R. He, K. T. Rim, T. Schiros, K. S. Kim, H. Zhou, C. Gutiérrez, S. P. Chockalingam, C. J. Arguello, L. Pálová, D. Nordlund, M. S. Hybertsen, D. R. Reichman, T. F. Heinz, P. Kim, A. Pinczuk, G. W. Flynn, and A. N. Pasupathy, Science **333**, 999 (2011).
[14] J. Ma, A. Michaelides, D. Alfè, L. Schimka, G. Kresse, and E. Wang, Phys. Rev. B **84**, 033402 (2011).
[15] K. Xu, P. Cao, and J. R. Heath, Science **329**, 1188 (2010).
[16] W. Gao and A. Tkatchenko, Phys. Rev. Lett. **114**, 096101 (2015).
[17] S. Dong, A. Zhang, K. Liu, J. Ji, Y. G. Ye, X. G. Luo, X. H. Chen, X. Ma, Y. Jie, C. Chen, X. Wang, and Q. Zhang, Phys. Rev. Lett. **116**, 087401 (2016).
[18] D. Wang, G. Chen, C. Li, M. Cheng, W. Yang, S. Wu, G. Xie, J. Zhang, J. Zhao, X. Lu, P. Chen, G. Wang, J. Meng, J. Tang, R. Yang, C. He, D. Liu, D. Shi, K. Watanabe, T. Taniguchi, J. Feng, Y. Zhang, and G. Zhang, Phys. Rev. Lett. **116**, 126101 (2016).
[19] V. A. Parsegian, *van der Waals Forces: A Handbook for Biologists, Chemists, Engineers and Physicists* (Cambridge University Press, Cambridge, UK, 2005).
[20] J. Rafiee, X. Mi, H. Gullapalli, A. V. Thomas, F. Yavari, Y. Shi, P. M. Ajayan, and N. A. Koratkar, Nat. Mater. **11**, 217 (2012).
[21] C.-J. Shih, Q. H. Wang, S. Lin, K.-C. Park, Z. Jin, M. S. Strano, and D. Blankschtein, Phys. Rev. Lett. **109**, 176101 (2012).
[22] Z. Li, Y. Wang, A. Kozbial, G. Shenoy, F. Zhou, R. McGinley, P. Ireland, B. Morganstein, A. Kunkel, S. P. Surwade, L. Li, and H. Liu, Nat. Mater. **12**, 925 (2013).
[23] X. Li, H. Qiu, X. Liu, J. Yin, and W. Guo, Adv. Funct. Mater. **27**, 1603181 (2017).
[24] E. M. Lifshitz, Sov. Phys. JETP **2**, 73 (1956).
[25] S. Grimme, J. Antony, S. Ehrlich, and H. Krieg, J. Chem. Phys. **132**, 154104 (2010).
[26] A. Tkatchenko and M. Scheffler, Phys. Rev. Lett. **102**, 073005 (2009).
[27] W. G. Hoover, *Molecular Dynamics* (Springer, Berlin, 1986).
[28] S. Tsoi, P. Dev, A. L. Friedman, R. Stine, J. T. Robinson, T. L. Reinecke, and P. E. Sheehan, ACS Nano **8**, 12410 (2014).
[29] J.-L. Li, J. Chun, N. S. Wingreen, R. Car, I. A. Aksay, and D. A. Saville, Phys. Rev. B **71**, 235412 (2005).
[30] J. Harl and G. Kresse, Phys. Rev. B **77**, 045136 (2008).
[31] S. Lebègue, J. Harl, T. Gould, J. G. Ángyán, G. Kresse, and J. F. Dobson, Phys. Rev. Lett. **105**, 196401 (2010).
[32] T. Björkman, A. Gulans, A. V. Krasheninnikov, and R. M. Nieminen, J. Phys.: Condens. Matter **24**, 424218 (2012).
[33] J. Harl and G. Kresse, Phys. Rev. Lett. **103**, 056401 (2009).
[34] G. Kresse and J. Furthmüller, Phys. Rev. B **54**, 11169 (1996).
[35] J. P. Perdew, K. Burke, and M. Ernzerhof, Phys. Rev. Lett. **77**, 3865 (1996).
[36] See Supplemental Material at http://link.aps.org/supplemental/10.1103/PhysRevB.97.241411 for supplemental data, additional technical details, and a convergence test for k-point sampling.
[37] E. H. Hwang and S. Das Sarma, Phys. Rev. B **75**, 205418 (2007).
[38] A. G. Marinopoulos, L. Reining, A. Rubio, and V. Olevano, Phys. Rev. B **69**, 245419 (2004).
[39] C. D. Spataru and F. Leónard, Phys. Rev. Lett. **104**, 177402 (2010).
[40] L. Yang, Nano Lett. **11**, 3844 (2011).
[41] A. Tkatchenko, Jr., R. A. DiStasio, R. Car, and M. Scheffler, Phys. Rev. Lett. **108**, 236402 (2012).
[42] X. Liu, J. Hermann, and A. Tkatchenko, J. Chem. Phys. **145**, 241101 (2016).
[43] A. Ambrosetti, A. M. Reilly, Jr., R. A. DiStasio, and A. Tkatchenko, J. Chem. Phys. **140**, 18A508 (2014).
[44] A. Ambrosetti, N. Ferri, Jr., R. A. DiStasio, and A. Tkatchenko, Science **351**, 1171 (2016).
[45] W. Liu, F. Maass, M. Willenbockel, C. Bronner, M. Schulze, S. Soubatch, F. S. Tautz, P. Tegeder, and A. Tkatchenko, Phys. Rev. Lett. **115**, 036104 (2015).
[46] J. Camarillo-Cisneros, W. Liu, and A. Tkatchenko, Phys. Rev. Lett. **115**, 086101 (2015).